A TEST CALCULATION ON SF_6 OF MODEL POTENTIALS FOR CORRELATION AND POLARIZATION EFFECTS IN POSITRON SCATTERING FROM MOLECULES

Robert R. Lucchese
Department of Chemistry, Texas A&M University, College Station, TX 77843-3255, USA
lucchese@mail.chem.tamu.edu

F. A. Gianturco
Department of Chemistry, The University of Rome, Cittá Universitaria, 00185 Rome, Italy

P. Nichols and Thomas L. Gibson
Department of Physics, Texas Tech University, P. O. Box 4180, Lubbock, TX 79409-1051, USA

Abstract Model local potentials that have been used to describe the correlation and polarization interactions in positron-molecule scattering are compared. Model density functional correlation-polarization potentials developed for electron-molecule and positron-molecule scattering are considered in addition to the distributed positron model. Results computed using these potentials are compared to available experimental data for positron-SF_6 scattering. It is found that the distributed positron model gives very good agreement with experimental data in contrast to the poor agreement found with the positron-molecule correlation-polarization potential.

1. Introduction

The study of low-energy positron scattering from molecules has a long history related to the interest in positron annihilation in gases and in

the slowing down of positrons in several media [1, 2]. Such investigations are in part motivated by the possible analytical applications of positrons, which include [3] surface analysis, microscopy of materials, and medical tomography [4]. In each case the cross sections from various elastic, inelastic, and reactive scattering processes are important in determining the resolution and contrast possible in the analytical application of positrons.

A more fundamental motivation for studying positron scattering from molecules is to compare the scattering cross sections to those of corresponding electron scattering processes [5, 6]. This comparison can then lead to a better understanding of the scattering process in these systems. For elastic scattering, the effective optical potential for positron and electron scattering from molecules can be decomposed into four components. The static part of the potential is due to the electrostatic interaction of the projectile with the unperturbed atomic or molecular electron density and the nuclei. The static potential has the same magnitude but has the opposite sign in the electron and positron cases. This interaction is almost everywhere attractive in the electron-molecule case and is thus repulsive in the positron case. In electron-molecule scattering there is also an attractive exchange interaction that is due to the antisymmetrization requirements in the many-electron wave function. This term is not present for positrons. The third term is the correlation-polarization (CP) potential which is caused by the response of the target to the presence of the projectile. At large separations between the projectile and the molecular target, the polarization potential is due to the static polarizability of the target and is the same for electrons and positrons. At shorter range, however, the effect of correlation between the projectile and the electrons of the target will be different for electron and positrons, but in both cases it gives rise to an attractive interaction.

One major difference between electron and positron scattering is that in the latter case there is the possibility of positronium (Ps) formation. The threshold for positronium formation, E_{Ps}, is given by $E_{\mathrm{Ps}} = E_{\mathrm{i}} - B_{\mathrm{Ps}}$, where E_{i} is the ionization energy of the molecule and B_{Ps} is the binding energy of Ps (6.8 eV). Above this threshold, the cross section for Ps formation can be a substantial fraction of the total scattering cross section [7]. An additional channel in positron scattering, which is not present in electron scattering, is direct positron annihilation, but this process has a small cross section except very near the threshold for Ps formation [8]. Thus, when comparing computed elastic positron scattering cross sections to measured total positron scattering cross sections, one would expect agreement between theory and experiment below E_{Ps},

with the elastic cross section being somewhat smaller than the total cross section above $E_{\rm Ps}$.

A commonly occurring feature in electron-molecule scattering is the shape resonance. They are one-electron resonances which generally occur due to a combination of the overall attractive interaction between the scattered electron and the molecule and the dynamical coupling between angular and radial motion of the projectile [9]. In atomic systems this dynamical coupling can be expressed as an effective radial potential which has a repulsive term that depends on the angular momentum and an attractive term due to the attractive electron-atom interaction. Because of the repulsive static interaction in positron-molecule scattering, one can only get traditional angular-momentum shape resonance when the CP potential is sufficiently attractive. It is also possible to have a resonance with the positron trapped inside a cage molecule, such as C_{60}, due to the electrostatic barrier provided by such a molecule. We have predicted shape resonances of both types in positron-C_{60} scattering based on local model potentials for the CP interaction [10]. The earlier calculations on C_{60} also showed that there are substantial differences between different models of the correlation potential. Unfortunately, there are as yet no experimental data for the positron-C_{60} scattering problem with which to distinguish the accuracy of the different potentials for large molecular systems such as C_{60}.

The study presented here examines the utility of different local CP potentials on a large system for which there are experimental data. We will consider three types of CP potentials. First, we will consider one that has been found to give good results for electron-molecule collisions [11] based on the Perdew-Zunger density-functional potential [12]. We will refer to this potential as the electron correlation-polarization (ECP) potential. The second potential is a density-functional potential that was developed for positrons interacting with a uniform electron gas by Boronski and Nieminen [13]. We will refer to this potential as the positron correlation-polarization (PCP) potential. The third potential is the distributed positron model (DPM). This local model potential was developed to provide an approximate (though accurate), non-empirical method to calculate the polarization potential for use in theoretical treatments of low-energy positron collisions with atoms [14] or molecules [15]. The total elastic positron scattering cross sections for these different CP potentials are then compared to the experimental data of Dababneh *et al.* [5] and Sueoka *et al.* [16] for positron-SF_6 scattering.

Positron-SF_6 scattering has been previously studied theoretically using a simple additive optical potential [17]. This model gave agreement with measured total scattering cross sections for collision energies above

200 eV. However, these results are not directly comparable to the elastic scattering cross sections computed here due to the inclusion of terms in the optical potential that incorporated inelastic scattering and Ps formation in the model.

2. The Theoretical Models

The full treatment of the positron-molecule problem would require the inclusion of the degrees of freedom due to nuclear motion, i. e. the rotational and vibrational motion of the molecule. As a first approximation, we will ignore the vibrational motion and assume that the molecule has a fixed geometry. Additionally, we will assume that the effect of the rotational motion is to average the cross section over the possible orientations of the molecule. These assumptions for positron scattering are commonly referred to as the fixed-nuclei (FN) approximation.

The static interaction, $V_{\rm S}(\mathbf{r}_p)$, was obtained from the electron density of the self-consistent-field (SCF) wave function of the target molecule at its equilibrium geometry. The most direct approach to the inclusion of positron-electron correlation usually involves an extensive configuration-interaction (CI) expansion of the target electronic wave function over a suitable set of excited electronic configurations with further improvement of the wave function obtained by adding Hylleraas-type functions which can describe the positron wave function within the physical space of the target electronic charge distribution [18]. Such expansions, however, are markedly energy-dependent and usually converge too slowly to be a useful tool for general implementation for complex molecular targets, where truncated expansions need to be very large before they begin to be realistic in describing correlation effects [19, 20]. As a consequence, we have developed approximate one-particle optical potentials for the treatment of the positron scattering problem that include the CP effects.

2.1. The ECP and PCP Potentials

As noted above, the asymptotic form of the polarization interaction is independent of the sign of the charge of the projectile and, in its simpler spherical form, is given by the well-known second-order perturbation expansion formula in atomic units

$$V_{\rm P}(\mathbf{r}_p) = \sum_{l=1}^{\infty} -\frac{\alpha_l}{2r_p^{2l+2}}, \tag{1}$$

where r_p represents the scalar positron distance from the molecular center of mass, and the α_l are the multipolar static polarizabilities of the molecule, which depend on the nuclear coordinates and on the elec-

tronic state of the target. In most cases only the lowest order is kept in the expansion given in Eq. (1) and therefore the target distortion is viewed as chiefly resulting from the induced dipole contribution, with the molecular dipole polarizability as its coefficient [20]. The drawback of the above expansion, however, is that it fails to correctly represent the short-range behavior of the full interaction and does not contain any effect from either static or dynamic correlation contributions [21]. We have therefore studied the use of the local density-functional approximation [22, 23, 24, 25] in order to correct for such failures. We assume that the dynamic correlation effects that dominate the short-range behavior of the CP potential, $V_{\rm CP}(\mathbf{r}_p)$, for closed-shell molecular targets can be treated using a density-functional theory (DFT) approach within the range of the target electronic density and can be further connected with the asymptotic dipolar form of Eq. (1) in the long range region.

We therefore describe the full $V_{\rm CP}(\mathbf{r}_p)$ interaction as given by two contributions which are connected at a distance r_p^c [22],

$$V_{\rm CP}(\mathbf{r}_p) = \begin{cases} V_{\rm C}^{\rm DFT}(\mathbf{r}_p) & |\mathbf{r}_p| \leq r_p^c \\ \\ V_{\rm P}(\mathbf{r}_p) & |\mathbf{r}_p| > r_p^c \end{cases} . \tag{2}$$

Furthermore, as discussed earlier [22], the short-range correlation contributions in Eq. (2) can be included either by considering the correlation effects on an homogeneous electron gas without reference to the positron projectile, as presented in Ref. [26], or by considering explicitly the positron projectile as an impurity within the homogeneous electron gas [13]. We have explicitly derived both forms of $V_{\rm CP}$ and discussed their merits for molecular targets in our earlier work. Both models will be employed in the present work. The potential based on the homogeneous electron gas will be that proposed by Perdew and Zunger [12] and will be denoted $V_{\rm ECP}(\mathbf{r}_p)$. The form based on the density-functional theory for an isolated positron interacting with an electron gas will be denoted $V_{\rm PCP}(\mathbf{r}_p)$ and is a modified version of the PCP2 potential proposed by Jain [27], which was derived from the density-functional energy expression of Boronski and Nieminen [13]. We have modified this potential to cut off the potential smoothly as $r_s \to \infty$ by using the function

$$V_{\rm C}(r_s) = \frac{1}{2}\left\{\frac{5.7382}{r_s^2} - \frac{3.5845}{r_s}\right\}, \tag{3}$$

where $r_s \geq 4.0$. The total interaction potential is then given as the sum of the static and CP potentials to yield

$$V_{\rm tot}(\mathbf{r}_p) = V_{\rm S}(\mathbf{r}_p) + V_{\rm CP}(\mathbf{r}_p), \tag{4}$$

where $V_{\rm CP}$ is either $V_{\rm ECP}$ or $V_{\rm PCP}$ as discussed above. The $V_{\rm P}$ potential was obtained using distributed polarization centers [9] with added terms so that $V_{\rm P}(\mathbf{r}_p) = V_{\rm C}(\mathbf{r}_p)$ when $|\mathbf{r}_p| = r_p^c$.

The connection radius, r_p^c, was obtained in a somewhat different manner than in previous studies [10], where r_p^c was taken to be the location of the intersection of the $l = 0$ partial waves of $V_{\rm C}$ and $V_{\rm P}$ which was closest to the origin. Additionally, if there was no intersection, then the location of the closest relative approach of the two potentials was taken. In the present study, we found that a more reasonable choice was to take the innermost intersection or closest relative approach of the two potentials along the ray from the center of mass of the molecule (the S atom) through one of the F atoms.

In $V_{\rm ECP}$ and $V_{\rm PCP}$ potentials, the actual connection of the potentials is done using a smooth switching function [28]. In this switching function there are four parameters, α, α', β, and β', which define the shape and range of the switching function. We have found that a satisfactory switching function can be defined in terms of a single switching distance d where $\alpha = 0.5493/d$, $\alpha' = \alpha/d^2$, $\beta = 0.8047/d^2$, and $\beta' = \beta/d^2$. For all calculations presented here we took $d = 0.25$ au.

2.2. The DPM Polarization Potential

The DPM potential is another approximate CP potential. This is based on a modification of the adiabatic polarization approach [29, 30] which makes use of quantum chemistry technology to provide a variational estimate of the polarization potential. In the adiabatic approximation to the polarization potential, the positron is treated as an additional "nucleus" (a point charge of +1) fixed at location $\mathbf{r}_p$ with respect to the center of mass of the atomic or molecular target. The target electronic orbitals are allowed to relax fully in the presence of this fixed additional charge and the energy lowering due to the distortion is recorded. This energy lowering represents the adiabatic polarization potential at one point in space. Of course, in order to represent fully the spatial dependence of this interaction, many such points must be computed.

However, due to nonadiabatic and short-range correlation effects, e.g. virtual Ps formation, the adiabatic approximation can overestimate the strength of the polarization potential for smaller values of $|\mathbf{r}_p|$ where the positron has penetrated the target electronic charge cloud [29, 30]. The DPM corrects for this by treating the positron as a smeared out distribution of charge rather than as a point charge. The physical reasoning behind this approach can be explained in the following way. If the scattering particle really were an additional nucleus, a proton, then

the dominant short-range correlation effect would be virtual hydrogen atom formation into ground and excited states, and the delta function distribution of positive charge at the center of mass of this virtual system would be correct. But, for a Ps atom, the positive charge is not well localized at the center of mass. Thus, to mimic this effect in computing the polarization potential, we represent the positron as a spherical distribution of charge in our quantum chemistry code. This leads to a polarization potential that more nearly reflects the correct physics and that smoothly reduces to the correct result for larger values of $|\mathbf{r}_p|$.

The distortion of the molecular orbitals in the electronic structure code is driven by the nuclear attraction integrals that involve the positron,

$$I_{i,j}^{\mathrm{NAI}} = \langle \alpha_i(\mathbf{r}_e) \, | V(\mathbf{r}_e; \rho_{\mathrm{pos}}) | \, \beta_j(\mathbf{r}_e) \rangle \, , \tag{5}$$

where the interaction V between an electron and ρ_{pos} is given by

$$V(\mathbf{r}_e; \rho_{\mathrm{pos}}) = \int d^3r \, \rho_{\mathrm{pos}}(\mathbf{r}) \, \frac{-1}{|\mathbf{r}_e - \mathbf{r}|}. \tag{6}$$

For the adiabatic approximation, $\rho_{\mathrm{pos}}(\mathbf{r}) = \delta(\mathbf{r} - \mathbf{r}_p)$, which is appropriate for the positive charge distribution in a virtual hydrogen atom and results in the standard nuclear attraction integrals.

The representation of the positron charge within the DPM is chosen to reflect the mean distribution of positive charge within virtual Ps atoms in the various states which can be formed. Although there is no precise data that would allow us to fix the size of the distribution, this parameter has never been treated as a "tunable parameter." We do not suggest that our choice of ρ_{pos} is by any means an exact representation when the virtual Ps is part of an atomic or molecular target, merely a physically reasonable one that automatically reduces to the adiabatic result in the appropriate region. In earlier studies [14, 15] of positron scattering involving the DPM we initially chose convenient, uniform spherical charge distributions whose radius R_p was set to either the average ground state Ps radius of 1.5 au or to 1.0 au, the maximum in the ground state Ps radial distribution with respect to the Ps center of mass. Both choices provided enormous improvement over scattering results obtained with the simple adiabatic approximation and strongly suggest that the DPM mimics the correct physics for short-range correlation.

As originally implemented the DPM scheme made use of direct three-dimensional quadrature to compute the modified nuclear attraction integrals of Eq. (5) so that, if necessary, essentially any choice of ρ_{pos} could be accommodated. However, to implement the DPM scheme for larger target molecules such as SF_6 (and in light of the success of the

very simple choices for the positron charge distribution) we now construct $\rho_{\rm pos}$ from the STO-3G basis for $1s$ atomic hydrogen with Slater exponent $\zeta = 1.24$. This choice gives results similar to those obtained with the DPM R_p=1.5 au distribution, but has the advantage that all of the modified nuclear attraction integrals can be evaluated in closed form by means of the very efficient functions used to compute two-electron integrals. Again, once the DPM potential is calculated, it is combined with the static potential to yield a total interaction potential as given by Eq. (4).

2.3. Solution of the Scattering Equations

By employing one of the forms of $V_{\rm tot}$ discussed above, we have reduced the positron-molecule scattering problem to a potential scattering problem, where the potential is a local potential but does not have spherical symmetry. The corresponding scattering equations are solved by expanding the Hamiltonian and the wave functions using a single-center expansion (SCE). This expansion reduces the Schrödinger equation to a set of coupled ordinary differential equations of the form

$$\left\{\frac{1}{2}\frac{d^2}{dr_p^2} - \frac{l(l+1)}{2r_p^2} + E_{\rm coll}\right\} f_{hl}^{p\mu}(r_p) = \sum_{h'l'} V_{hl,h'l'}^{p\mu}(r_p) f_{h'l'}^{p\mu}(r_p), \qquad (7)$$

where $E_{\rm coll}$ is the collision energy and the positron continuum radial functions $f_{h'l'}^{p\mu}(r_p)$ are the required unknown quantities originating from the symmetry-adapted SCE form of the wave function of the scattered particle,

$$F_{p\mu}(\mathbf{r}_p) = \sum_{hl} r_p^{-1} f_{hl}^{p\mu}(r_p) X_{hl}^{p\mu}(\hat{r}_p). \qquad (8)$$

Here $(p\mu)$ labels the relevant irreducible representation (IR), with p describing the IR of the scattered positron and with μ being one of its components, and $X_{hl}^{p\mu}(\hat{r}_p)$ are the generalized harmonics. The index h further labels a specific angular basis function for each chosen partial wave contribution l found in the pth IR under consideration. The coupling matrix elements on the right-hand side of Eq. (7) are then given by

$$V_{hl,h'l'}^{p\mu}(r_p) = \langle X_{hl}^{p\mu} | V_{\rm tot}(\mathbf{r}_p) | X_{h'l'}^{p\mu} \rangle. \qquad (9)$$

The details of the angular products have been described before [31] and will therefore not be repeated here. Suffice it to say that, when using the static-correlation-polarization interaction within the SCE formulation and the close-coupling approximation implied by Eq. (7), the formulation and the corresponding coupled-differential equations are solved

to yield rotationally summed, integral elastic cross sections for each IR contributing to the scattering process. The total cross section is then given as

$$\sigma_{\rm tot}(E_{\rm coll}) = \sum_{p,\mu} \sigma^{\rm el}_{p,\mu}(E_{\rm coll}). \tag{10}$$

One should stress at this point that the above treatment does not include any contribution from a number of processes: Ps formation, direct positron annihilation, electronic excitation, ionization, vibrational excitation, or rotational excitation.

3. Comparison of the Results from the Different Potentials

For the computation of the static, ECP, and PCP potentials, for positron-SF_6 scattering we used a 6-311++G(3df) one-electron basis set [32] which yielded a self-consistent field energy of -994.309353 au for R(S – F) = 2.948 au. The asymptotic polarizability was taken to be α = 4.50 Å^3 [33, 34], which was distributed with 0.36 Å^3 centered on the S atom and 0.69 Å^3 on each of the F atoms.

The DPM polarization potential was obtained from the PATMOL [35] suite of quantum chemistry codes using a triple zeta with double polarization basis [36] for the target. This basis consists of a (12s9p2d/7s5p2d) set on the S atom and (9s5p2d/5s3p2d) set on the F atoms. The ground state energy in this basis is -994.2489 au. Finally, for calculations involving the DPM potential, an additional (4s3p) basis set was centered on the positron location. Computations for the DPM polarization potential were performed on a 16-node Beowulf cluster [37] running Linux with standard MPI calls.

In Fig. 1 we show the different $V_{\rm CP}$ potentials along three different rays from the S atom outward. In the figures showing the potentials, the directions of the rays are given in terms of θ and ϕ, which are the usual spherical polar angles and where the SF_6 molecule is oriented with the S atom at the origin and with the six F atoms on the axes of the corresponding Cartesian coordinate system. As was noted earlier [10], the PCP potential is much more attractive than the ECP potential. Interestingly, the DPM potential is between these two potentials in strength. The DPM potential is much smoother near the nuclei than are the two density-functional CP potentials which reflect the sharp peak in the electron density at the nuclei. In Fig. 2 we give the values of $V_{\rm tot}$ for these three potentials. Note in this figure the small spikes in the static potential in the directions that do not pass through one of the F atoms. These features are due to the truncated partial wave expansions and would not

be present in the limit of an infinite expansion. One can see that, on the scale used in Fig. 2, the ECP and DPM potentials are very similar whereas the PCP potential is substantially more attractive than either the ECP or DPM potentials. Another important point illustrated in Fig. 2 is that the part of the CP potential further than 1.0-1.5 au from the nearest nucleus will have the most significant effect on the scattering properties of the molecule since in regions nearer to the nuclei the repulsive static interaction is dominant.

Although it is not apparent in Figs. 1 and 2, the ECP and DPM potentials have different asymptotic strengths. The ECP was fixed to agree asymptotically with the experimental static electronic polarizability of SF_6, which is $\alpha = 4.50$ Å^3 [33, 34], whereas the polarizability found in the DPM calculations was $\alpha = 3.50$ Å^3. In order to consider the sensitivity of the computed cross section to the asymptotic polarizability, we also constructed an ECP potential which used the same asymptotic polarizability as was computed in the DPM potential. We will refer to this potential as the ECP2 potential. In Fig. 3 we show the ECP, ECP2, and DPM potentials along the ray from the S atom through one of the F atoms ($\theta = 90°$ and $\phi = 0°$) in the range of r_p where there is a substantial dependence on the manner in which the V_C and V_P are joined together. By changing the asymptotic strength of the potential, the value of r_p^c changed from 6.22 au in the ECP potential to 5.81 au in the ECP2 potential. Thus, to separate the effect of the changing asymptotic potential from the change in the connection radius we have also considered a third ECP potential, ECP3, which was obtained using the same value of the polarizability as was used in the ECP potential, but fixing the connection radius to be 5.81 au as was found in the ECP2 potential. The value of this potential is also shown in Fig. 3. One can see that ECP2 and ECP3 are nearly identical in the region shown in Fig. 3, with only small absolute differences due to the different asymptotic strength.

In Fig. 4, the values of the three ECP potentials and the DPM potential are shown on the ray with $\theta = 45°$ and $\phi = 45°$. We can see that in this direction the ECP and ECP3 potentials are nearly the same. Thus, there is little sensitivity to the value of r_p^c. Also in this direction, the ECP2 potential is a smooth connection of the ECP potentials at small r_p and the asymptotic form of the DPM potential.

The total elastic scattering cross sections for these potentials are given in Fig. 5. Considering that the ionization potential of SF_6 is 15.3 eV [38] and that the binding energy of Ps is 6.8 eV, the threshold for Ps formation in this system is 8.5 eV. Thus, one would expect reasonable agreement between theoretical elastic cross sections and experimental total cross sections for energies less than 8.5 eV. In Fig. 5 we see that

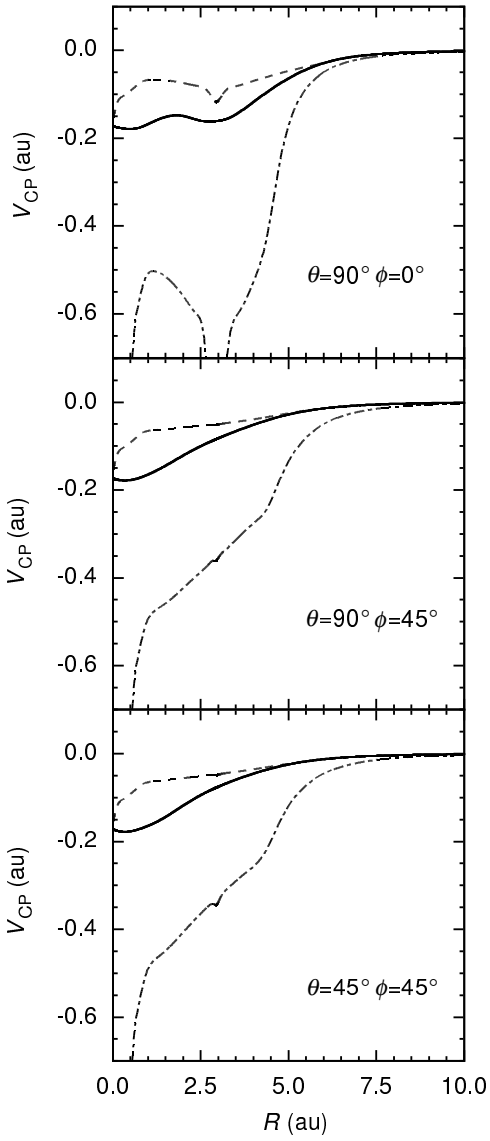

Figure 1. The CP potentials in the directions indicated: the solid line is the DPM potential; the dashed line is the ECP potential; the dot-dashed line is the PCP potential.

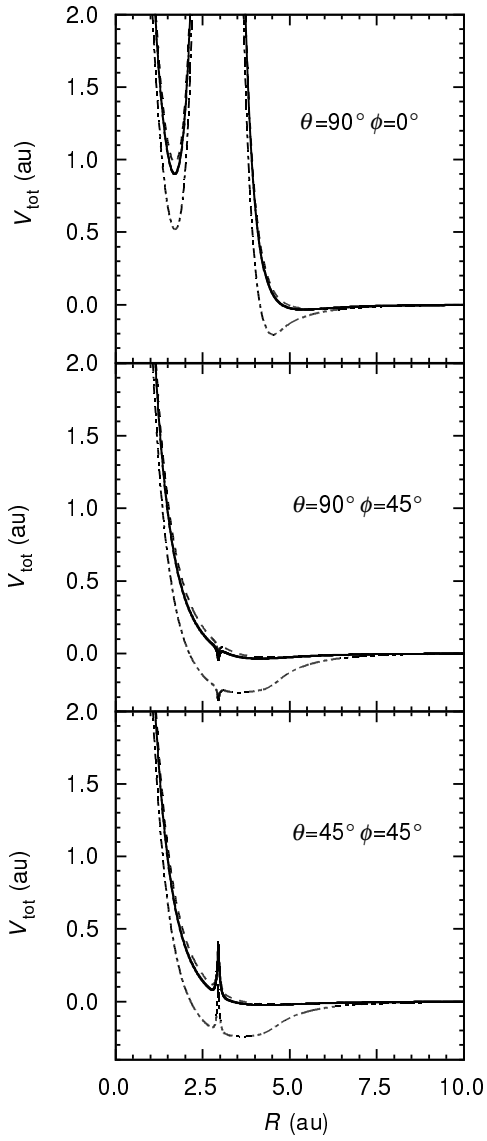

Figure 2. The $V_{\rm tot}$ potentials in the directions indicated: the solid line is the DPM potential; the dashed line is the ECP potential; the dot-dashed line is the PCP potential.

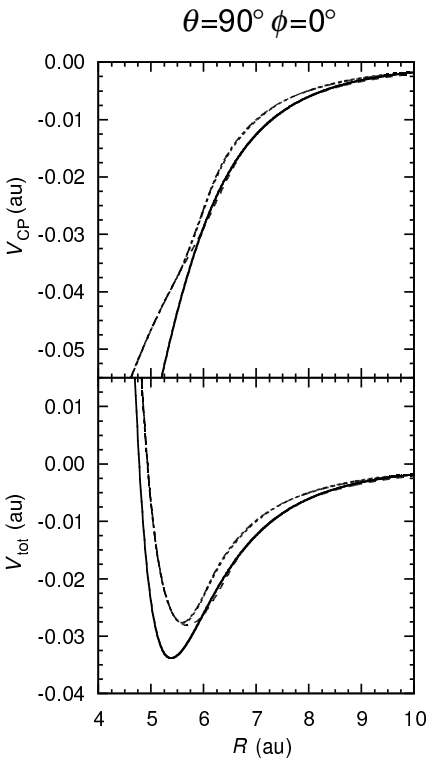

Figure 3. The $V_{\rm CP}$, $V_{\rm tot}$ potentials in the $\theta = 90^\circ$ $\phi = 0^\circ$ direction: the solid line is the DPM potential; the long-dashed line is the ECP potential; the short-dashed line is the ECP2 potential; the dot-dashed line is the ECP3 potential.

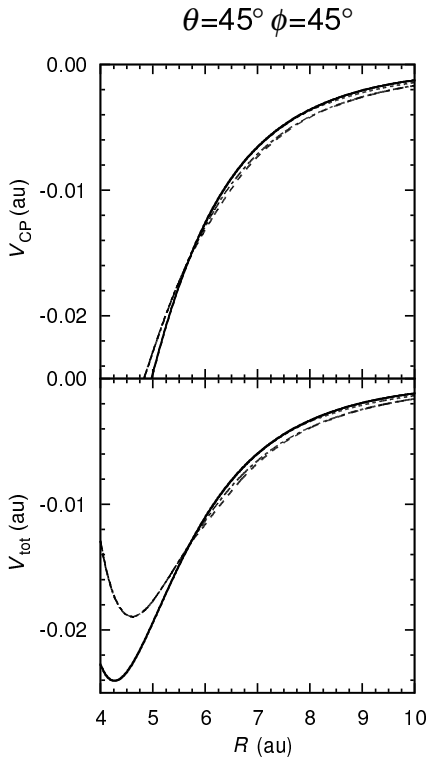

Figure 4. Value of the $V_{\rm CP}$, $V_{\rm tot}$ potentials in the $\theta = 45^\circ$ $\phi = 45^\circ$ direction: the solid line is the DPM potential; the long-dashed line is the ECP potential; the short-dashed line is the ECP2 potential; the dot-dashed line is the ECP3 potential.

the DPM cross sections are in good agreement with the experimental data below a scattering energy of 8.5 eV. In Fig. 6 an expanded view of the low energy portion of the results is given where it is seen that there is particularly good agreement between the DPM calculations and the data of Sueoka *et al.* [16].

The difference between the ECP and ECP3 calculations gives an indication of the sensitivity of the computed cross sections to the connection radius. In Fig. 5 we can see that at very low energy the change in r_p^c leads to a 30% change in the cross section. Above $\sim$1 eV the difference is much smaller. The difference between the ECP2 and ECP3 results from the different asymptotic potential used in each case. Also from Fig. 5 we see that the low energy cross sections are most sensitive to the change in the asymptotic potential. Above $\sim$10 eV all three ECP potentials give very similar results. The ECP potentials represent the strength of correlation effects in electron-molecule scattering. Thus the difference

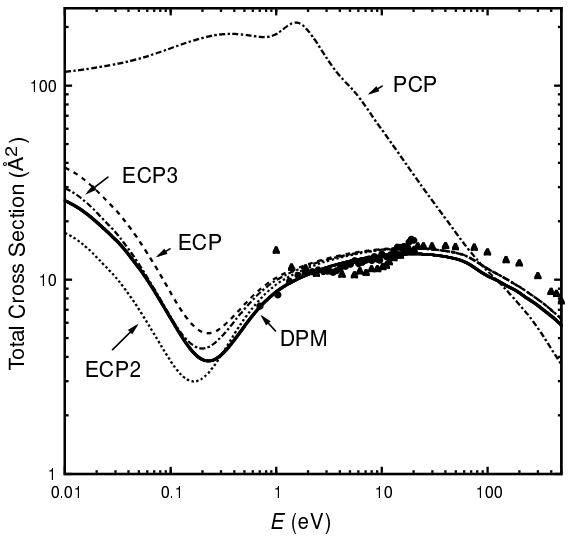

Figure 5. Total positron-molecule scattering cross sections for the potentials indicated: the circles are from Sueoka et al. [16]; the triangles are from Dababneh et al. [5]. For both experiments, the uncertainties given in the original paper are smaller than the size of the symbols used in the figure.

between the ECP and DPM results above ∼10 eV can be ascribed to the difference in short-range correlation effects for positron and electron scattering.

Finally we note that the results obtained with the PCP potential are substantially different from the experiment and also from the results obtained with the other potentials. One can observe a feature at ∼1.5 eV that is due to a shape resonance in the PCP calculation. As in the positron-C_{60} study [10], such a feature seems to be the result of the overly attractive nature of the PCP potential.

A previous study on positron scattering from CF_4 and CCl_4 [39] has shown that it is possible to obtain reasonable agreement between experimental cross sections and those calculated using the PCP potential. However, to get such agreement required a very different choice for the V_P potential. In the earlier study [39] V_P was constructed using all of the polarizability located on the central C atom. The connecting radius, r_p^c, was then between the C atom and the halogen atoms. This choice of V_P and r_p^c effectively eliminated the overly attractive PCP in the region of the halogen atoms leading to reasonable agreement between experiment and theory.

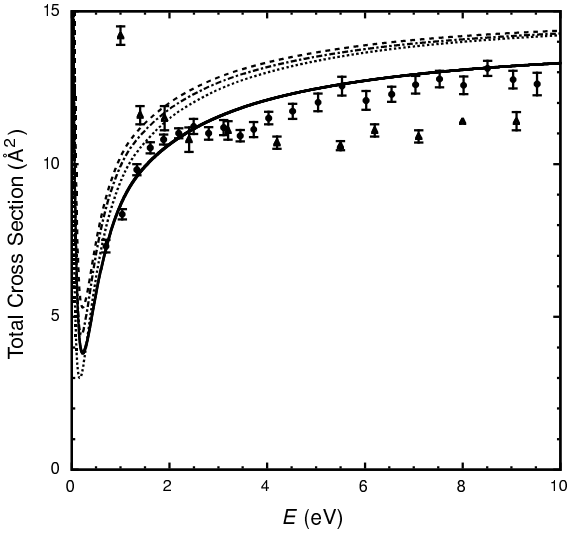

Figure 6. Total positron-molecule scattering cross sections: the solid line gives the results of the DPM potential; the long-dashed line gives the results of the ECP potential; the short-dashed line gives the results of the ECP2 potential; the dot-dashed line gives the results of the ECP3 potential; the circles are from Sueoka *et al.* [16]; the triangles are from Dababneh *et al.* [5].

4. Conclusions

The scattering cross sections obtained using the DPM potential for positron-SF_6 scattering are in very good agreement with the most recent experimental data. The DPM potential does have one empirical parameter, ζ, however the good agreement for scattering cross sections found here in SF_6 with a value of $\zeta = 1.24$, chosen to represent the distribution of positive charge in isolated Ps, suggests that a single value of ζ may lead to accurate model CP potentials independent of the molecule studied.

The ECP potentials can yield cross sections that are fairly close to the experimentally measured values. However, the results one obtains in positron-molecule scattering are much more sensitive to how the V_C and V_P potentials are connected than in the electron scattering case. This is most likely due to the fact that, in positron scattering, the static potential and the CP potentials have opposite signs. Thus, the net potential is smaller in magnitude than either the static or CP potentials, and small relative changes in the CP potential yield larger relative changes in the total potential [39]. A second source of sensitivity to the connection method is that near the nuclei the total positron-molecule potential is

very repulsive. Thus, the scattering cross section is insensitive to the value of the correlation potential in the region of the nuclei but is very sensitive to the CP potential in the region outside the nuclei, as seen in Fig. 3. The part of the CP potential which has an impact on the scattering cross section is the region where the connection occurs. This leads to the unsatisfactory sensitivity to the connection parameters used to construct ECP type potentials and limits their utility in a predictive model for positron-molecule scattering.

The PCP potential as implemented here does not lead to satisfactory results. However a different choice of $V_{\rm P}$ can lead to better agreement with experimental data [39]. This sensitivity to the form of the asymptotic potential in the PCP potentials again highlights the need to find a better way to connect the $V_{\rm P}$ and $V_{\rm C}$ potentials if one wants to employ potentials of this type.

Finally, we note that the an adiabatic positron-molecule CP potential, denoted $V_{\rm pscf}$ in Ref. [39], has been applied to positron scattering from CF_4 and CCl_4. That previous study found that the the $V_{\rm pscf}$ potential gave better agreement with experimental data than did the PCP potential even with the different choice of connecting to $V_{\rm P}$. A direct comparison of the adiabatic and DPM type interaction potentials for larger molecular systems would be of interest.

Acknowledgments

We are grateful to the NATO Scientific Division for the award of Collaborative Research Grant No. CRG950552, 922/94/JARC501. We also acknowledge the financial support of the Italian National Research Council (CNR) and the University of Rome Research Committee. R. R. L. wishes to thank the Welch Foundation (Houston) for its financial support under grant No. A-1020 and to acknowledge the support of the Texas A&M University Supercomputing Facility. T. L. G. and P. N. are also grateful for support from the Robert A. Welch Foundation under grant No. D-1316 and would like to thank Mr. Lee Burnside for his expertise in constructing and running our Beowulf cluster.

References

[1] H. J. Ache, ed., *Positronium and Muonium Chemistry* (Am. Chem. Soc., Washington D.C., 1979).

[2] A. Passner, C. M. Surko, M. Leventhal and A. P. Mills Jr., Phys. Rev. A **39**, 3706 (1989).

[3] P. Coleman, ed., *Positron Beams and Their Applications* (World Scientific, Singapore, 2000).

[4] G. L. Brownell, T. F. Budinger, P. C. Lauterbur, and P. L. McGeer, Science **215**, 619 (1982).

[5] M. S. Dababneh, Y.-F. Hsieh, W. E. Kauppila, C. K. Kwan, S. J. Smith, T. S. Stein, and M. N. Uddin, Phys. Rev. A **38**, 1207 (1988).

[6] W. E. Kauppila and T. S. Stein, Adv. At. Molec. Opt. Phys. **26**, 1 (1990).

[7] G. Laricchia and M. Charlton, in *Positron Beams and Their Applications*, P. Coleman, ed. (World Scientific, Singapore, 2000), p. 41.

[8] G. Laricchia and C. Wilkin, Nucl. Instr. Meth. B **143**, 135 (1998).

[9] R. R. Lucchese and F. A. Gianturco, Intern. Rev. Phys. Chem. **15**, 429 (1996).

[10] F. A. Gianturco and R. R. Lucchese, Phys. Rev. A **60**, 4567 (1999).

[11] F. A. Gianturco, R. R. Lucchese, and N. Sanna, J. Chem. Phys. **102** 5743 (1995).

[12] J. P. Perdew and A. Zunger, Phys. Rev. B **23**, 5048 (1981).

[13] E. Boronski and R. M. Nieminen, Phys. Rev. B **34**, 3820 (1986).

[14] T. L. Gibson, J. Phys. B **23**, 767 (1990).

[15] T. L. Gibson, J. Phys. B **25**, 1321 (1992).

[16] O. Sueoka, H. Takaki, and A. Hamada, At. Collision Res. Japan **23**, 6 (1997).

[17] J. Sun, G. Yu, Y. Jiang, and S. Zhang, Eur. Phys. J. D **4**, 83 (1998).

[18] e. g. see: E. A. G. Armour, Phys. Rep. **169**, 2 (1988).

[19] R. N. Hewitt, C. J. Noble and B. H. Bransden, J. Phys. B **25**, 557 (1992).

[20] M. A. Morrison, Adv. At. Mol. Phys., **24**, 51 (1988).

[21] H. D. Meyer, Phys. Rev. A **40**, 5605 (1989).

[22] F. A. Gianturco, A. Jain and J. A. Rodriguez-Ruiz, Phys. Rev. A **48**, 4321 (1993).

[23] F. A. Gianturco and J. A. Rodriguez-Ruiz, Phys. Rev. A **47**, 1075 (1993).

[24] F. A. Gianturco and R. Melissa, Europhys. Lett. **33**, 661 (1996).

[25] F. A. Gianturco, J. A. Rodriguez-Ruiz, and N. Sanna Phys. Rev. A **52**, 1257 (1995).

[26] J. K. O'Connell and N. F. Lane, Phys. Rev. A **27**, 1893 (1983).

[27] A. Jain, Phys, Rev. A **41**, 2437 (1990).

[28] F. A. Gianturco and R. R. Lucchese, J. Chem. Phys. **111**, 6769 (1999).

[29] M. A. Morrison and P. J. Hay, Phys. Rev. A **20**, 740 (1979).

[30] D. G. Truhlar, D. A. Dixon, and R. A. Eades, J. Phys. B **12**, 1913 (1979).

[31] F. A. Gianturco and A. Jain, Phys. Rep. **143**, 347 (1986).

[32] W. J. Hehre, L. Radom, P. v. R. Schleyer, and J. A. Pople, *Ab Initio Molecular Orbital Theory* (Wiley, New York, 1986).

[33] J. M. St-Arnaud and T. K. Bose, J. Chem. Phys. **71**, 4951 (1979).

[34] G. Maroulis, Chem. Phys. Lett. **312**, 255 (1999).

[35] T. L. Gibson, "Positron-Matter Interactions Page," 26 June 2000, <http://www.phys.ttu.edu/~ritlg/research/pos1.html> (16 January 2001).

[36] A. Schäfer, H. Horn, and R. Ahlrichs, J. Chem. Phys. **97**, 2571 (1992).

[37] T. L. Sterling, J. Salmon, D. J. Becker, and D. F. Savarese, *How to Build a Beowulf: A Guide to the Implementation and Application of PC Clusters* (MIT Press, Cambridge, 1999).

[38] D. C. Frost, C. A. McDowell, J. S. Sandhu, and D. A. Vroom, J. Chem. Phys. **46**, 2008 (1967).

[39] R. Curik, F. A. Gianturco, and N. Sanna, J. Phys. B **33**, 615 (2000).